



Hematite and multi-walled carbon nanotubes stimulate a faster syntrophic pathway during methanogenic beet sugar industrial wastewater degradation

John Justo Ambuchi¹ · Zhaohan Zhang¹ · Yue Dong¹ · Linlin Huang¹ · Yujie Feng¹

Received: 22 September 2017 / Revised: 19 April 2018 / Accepted: 7 May 2018
© Springer-Verlag GmbH Germany, part of Springer Nature 2018

Abstract

The quest to understand and subsequently improve the role played by bacteria and archaea in the degradation of organic matter both in natural and engineered anaerobic ecosystems has intensified the utilization of nanoparticles. Microbial communities are known to syntrophically cooperate during the anaerobic conversion of substrates into methane gas via the direct exchange of electrons. In this study, the role of hematite (Fe₂O₃—750 mg/L) and multi-walled carbon nanotubes (MWCNTs—1500 mg/L) during the degradation of beet sugar industrial wastewater (BSIW) in a batch experiment was investigated. Hematite and MWCNTs enhanced methane gas generation by 35 and 20%, respectively. Furthermore, microbial syntrophic communities might have exchanged metabolic electrons more directly, with hematite and MWCNTs serving as electron conduits between the homoacetogens and methanogens, thereby establishing a direct interspecies electron transfer (DIET) pathway. Additionally, hematite and MWCNTs enriched the bacteria *Firmicutes* while *Chloroflexi* reduced in abundance. Scanning electron microscopy and confocal laser scanning microscopy demonstrated that extracellular polymeric substances had noticeable interactions with both hematite and MWCNTs. Our findings provide vital information for more understanding of the response of microbes to hematite and MWCNTs in a complex natural environment.

Keywords Beet sugar industrial wastewater · Direct interspecies electron transfer · Hematite · Methane gas · Multi-wall carbon nanotubes

Introduction

The successful degradation of organic matter in the methanogenic ecosystem is attributed to syntrophic interspecies electron exchange (Stams and Plugge 2009). During this process, microbial communities anaerobically convert complex organic matter into methane (CH₄) and carbon dioxide (CO₂) gases. The conversion of beet sugar industrial wastewater (BSIW) into CH₄ and CO₂ is an essential process (Bastviken et al. 2011; Smith and Mah 1978), and any effort towards improving this process is undoubtedly of great importance since the

high concentrations of hydrocarbons and sucrose therein (Angelidaki and Sanders 2004) increase the potential of methane gas production.

A substrate is first hydrolyzed into acetate, CO₂, and either H₂ or formate by the bacteria before the methanogenic microorganisms consume the electrons, reducing the CO₂ to CH₄ gas (Antoni et al. 2007). In this case, with BSIW as a substrate, invertase activity plays a crucial role in converting sucrose into glucose and fructose, where the latter is converted into glucose by isomerase enzymes. Glucose is subsequently fermented at low hydrogen partial pressures (< 10 Pa), where the released electrons shift fermentation patterns to produce acetate, CO₂, and hydrogen per the following reaction: Glucose + 2H₂O → 2Acetate + 2H⁺ + 2CO₂ + 4H₂ (ΔG^{o'} = -280 kJ/mol) (Schink 1997). These metabolic intermediates are syntrophically converted to CH₄ and CO₂ through different degradation pathways of electron transfer.

This essential mechanism of electron transfer is executed in three different ways. First, electron transfer can be aided by interspecies H₂ (or formate) transfer. During this process,

✉ Zhaohan Zhang
hitzzh@hit.edu.cn

✉ Yujie Feng
yujief@hit.edu.cn

¹ State Key Laboratory of Urban Water Resource and Environment, Harbin Institute of Technology, No. 73, Huanghe Road, Nangang District, Harbin 150090, China

microorganisms that require electron sinks participate in proton reduction to produce H₂, which is utilized as an electron donor towards consuming methanogenic archaea (Stams et al. 2006; Stams and Plugge 2009). However, this process is only viable if the concentrations of acetate and especially H₂ are kept at low levels by acetoclastic and hydrogenophilic methanogens (Stams et al. 2006; Thiele and Zeikus 1988). Formate can also play the same role as hydrogen (Boone et al. 1989; Thiele and Zeikus 1988).

Second, the *Geobacter metallireducens* and *Methanosaeta* species can make direct contact with each other, with the latter accepting electrons for the reduction of carbon dioxide to methane through direct interspecies electron transfer (DIET) (Rotaru et al. 2014). This might also occur between *Geobacter metallireducens* and *Geobacter sulfurreducens*, with the assistance of pili or cytochromes (Nagarajan et al. 2013).

Third, as established by recent studies, electrically conductive particles can stimulate DIET. The nanometer- to micrometer-sized materials serve as conduits for electron transfer between the electron donors and electron acceptors among the microbial consortia. For example, the direct exchange of electrons has been aided by (semi)conductive iron-oxide particles (hematite and magnetite) (Aulenta et al. 2013; Kato et al. 2012a, b; Li et al. 2015a; Viggli et al. 2014; Zhuang et al. 2015), as well as other electrically conductive materials and minerals, including activated carbon (Zhang et al. 2018) and single-wall carbon nanotubes (Li et al. 2015b).

This study aims to demonstrate that hematite and multi-walled carbon nanotubes (MWCNTs) are likely to provide a viable novel strategy for triggering DIET among syntrophic microbes, subsequently promoting a faster and robust conversion of BSIW into methane gas. In addition, the use of scanning electron microscopy (SEM) and confocal laser scanning microscopy (CLSM) observations could show interactions among the nanoparticles, microbes and extracellular polymeric substances (EPS), of which the latter is useful in establishing a protective defense against piercing by the hematite and MWCNTs, which could subsequently result in toxicity and subsequent inhibition of microbial activity. The composition of the microbial community was also analyzed. Given that conductive minerals are ubiquitous in nature, such interactions could be harnessed and utilized for the development of efficient bioenergy processes.

Materials and methods

Source of materials

The nanoparticles (NPs, composed of hematite and MWCNTs) utilized in this batch experiment were commercially obtained from Alpha Nano Technology Company

(Chengdu, China). The preparation of the stock suspension involved mixing the NPs with deionized water and 1 h of sonication (using a Sonicator-VCX130-USA) to ensure a homogeneous mixture of the particles. The inoculum was anaerobic granular sludge (AGS) obtained from a beer manufacturer (Harbin city, China). It was acclimated in an expanded granular sludge bed reactor (EGSB) with a volume of 6.5 l for 1 month using a substrate synthetically prepared, as previously described (Angelidaki and Sanders 2004), with sucrose as the main carbon source (2000 mg/L).

The reactors (250-mL glass serum bottles) were filled with 100 mL of inoculum and with 120 mL of a substrate of pH 6.8 ± 0.2 (after adjustment using lime) obtained from a Sugar Beet Factory (Nehe City, China). The characteristics of the substrate are shown in Table 1. The serum bottles without NPs were used as control reactors, while others were filled with hematite (750 mg/L) or MWCNTs (1500 mg/L). This procedure was carried out in duplicate. Thereafter, the bottles were sealed with rubber stoppers together with plastic screw caps, sparged with nitrogen gas for at least 10 min to maintain anaerobic conditions and immediately incubated at 36 ± 1 °C in a mechanical shaker at 150 rpm.

Analytical methods

Substrate samples, of 2–3 mL, used for the determination of soluble chemical oxygen demand (sCOD) and volatile fatty acids (VFAs) were collected 6 h after the start of the experiment and every 12 h thereafter. They were centrifuged for 5 min (13,000 rpm) and filtered using 0.45 µm pore-sized filters. A gas chromatograph (Agilent GC 7890A, USA) with a flame ionization detector (FID) and HP-INNOWAX column (HP-Innowax 19095N-123, Agilent, USA) was used for VFA

Table 1 Characteristics of beet sugar industrial wastewater (all units are in mg/L, apart from pH)

Parameter	Measurement
pH	6.8 ± 0.20
COD	2000 ± 150
SS	553 ± 77.78
VSS	260 ± 39.56
TOC	7579 ± 561.07
Cl ⁻	146.51 ± 78.39
SO ₄ ²⁻	99.76 ± 9.48
NO ₃ ⁻	54.24 ± 11.23
TP	4 ± 1.10
K	65.07 ± 10.31
Ca	225.55 ± 0.72
Na	197.05 ± 64.70
Mg	7.18 ± 1.29
Al	0.13 ± 0.11
Fe	0.26 ± 0.23

analysis. The same gas chromatograph was used to determine the composition of the biogas.

After the experiment, sludge granules were collected and stored immediately in a negative (−) 40 °C refrigerator, following which microbial community analysis was conducted using pyrosequencing with a Sangon agarose recovery kit from Sangon Biotech Co., Ltd. (Shanghai, China). Agarose gel was run to check the integrity and the concentration of the extracted genomic deoxyribonucleic acid (DNA). This was then quantified using the Qubit 2.0 DNA kit for the polymerase chain reaction (PCR) reaction. The PCR primer used was fused universal primer of the MiSeq sequencing platform. Additionally, agarose gel electrophoresis was carried out to test the PCR products and recover the DNA. This process was carried out based on the Sangon agarose recovery kit from Sangon Biotech Co., Ltd. (Shanghai, China). Thereafter, the sequences were phylogenetically assigned to the domain phylum, class, order, family, and genus as per the Bergeys taxonomic group using a Ribosomal Database Project naïve Bayesian ribosomal DNA classifier. The search for the closest matching nucleotide sequences in the GenBank database was carried out using the Blast program (<http://www.ncbi.nlm.nih.gov/BLAST/>).

During the microbial community analysis, samples of control, MWCNT, and hematite reactors were given barcodes AGAACA, GGTGTG, and AGAGAC yielding 19,955, 24,475, and 24,630 raw number of bacterial sequences, respectively. For the analysis of archaea, samples of control, MWCNT, and hematite reactors were given barcodes TCTGCGA, AGTCGAT, and AGCGTCT yielding 46,163, 40,544, and 35,035 raw number of sequences respectively. Sequences less than 300 bp in length were removed together with OUT target and chimeric sequences. This process of quality check generated filtered sequences (reads) as shown in Table 2. This was followed by classifying the qualified reads in taxonomic clusters using RDP's classifier (bootstrap cutoff of 50%) yielding the number of OTUs as given in column 3 of Table 2. This data set was then used to calculate index estimators such as Shannon index, Ace index, Chao1 index, Coverage, and Simpson.

All sequencing data obtained in this study were deposited in GenBank of the National Center for Biotechnology

Information (NCBI) with accession number of SUB3173876 (MG283324-MG287107), SUB3173968 (MG328901-MG333428), and SUB3173993 (MG367669-MG371978) for the original, hematite exposed, and multi-walled carbon nanotubes exposed sludge.

Multiple fluorescence staining of AGS and imaging

The sludge granules collected after the experiments were fixed with 2.5% glutaraldehyde in a phosphate-buffered saline of pH 7.2 for CLSM. This was followed by fluorescent staining with FITC, Con A, and calcofluor white (Invitrogen Life Science, USA) for proteins, α -D-glucopyranose polysaccharides, and β -D-glucopyranose polysaccharides, respectively, as described by Li et al. (2015b). Some sludge granules collected were also used for SEM analysis. The procedure for pretreatment, as described in the literature (Wang et al. 2007), was employed and was conducted using energy dispersive spectroscopy (EDS).

Results

Influence of hematite and MWCNTs on substrate degradation

The influences of hematite and MWCNTs on the removal efficiency of sCOD during the digestion of BSIW were analyzed (Fig. 1). It appears that the degradation of BSIW was substantially influenced by the presence of MWCNTs and or hematite, contrary to the control sample. The initial 6 h was characterized by control reactors with a higher COD removal efficiency. After the initial 6 h period, the hematite and MWCNT reactors achieved a rapid degradation of the substrate. This resulted in decreases in the concentrations of sCOD in the control, hematite, and MWCNT reactors with sCOD removal efficiency of 50.8, 54.2, and 64.2% after 54 h; 70.6, 84.2, and 82.1% after 78 h; and further to 89.7, 90.9, and 90.2% after 150 h, respectively. The results indicate that MWCNTs stimulated degradation of the substrate in a faster and more robust manner compared with hematite during the initial stages of anaerobic digestion (Fig. 1). As previously noted, slightly higher sCOD

Table 2 Various estimators for the evaluation of bacterial community diversity and richness in terms of Shannon, Ace, Chao1, Coverage, and Simpson for archaea and bacteria

	Sample	Reads	OTU	Shannon	ACE	Chao1	Coverage	Simpson
Archaea	Control	46,125	1084	3.020	2946.83	2174.6	0.988	0.178
	MWCNT	40,501	930	2.850	2654.92	1962.8	0.988	0.201
	Fe ₂ O ₃	35,021	893	2.874	2904.03	1977.7	0.986	0.188
Bacteria	Control	19,695	1421	5.194	3946.82	2971.7	0.963	0.0191
	MWCNT	24,193	1686	5.354	5340.31	3741.6	0.963	0.0148
	Fe ₂ O ₃	24,368	1552	5.276	4387.58	3114	0.968	0.0156

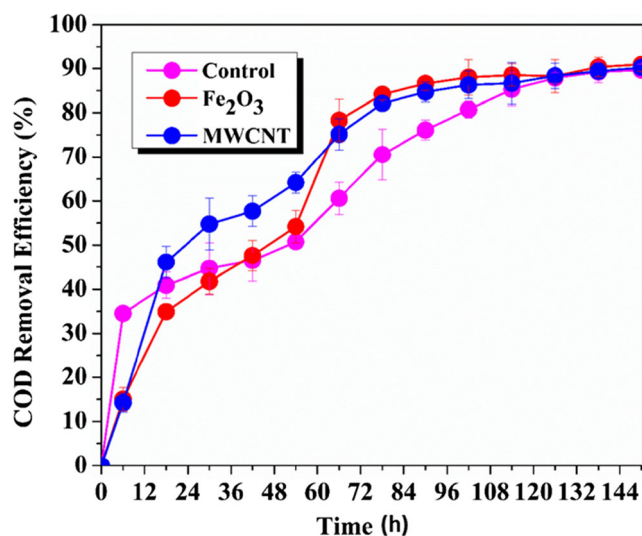


Fig. 1 Anaerobic degradation of beet sugar industrial wastewater (BSIW) in a batch experiment for control, hematite, and MWCNT reactors illustrating the changing profiles of COD, wherein the error bars represent the standard deviations of the duplicate tests

removal efficiency in the control reactors at the start of the experiment might have resulted from uninterrupted microbial activity, whereas the presence of nanoparticles may have altered the microorganisms' performance due to acclimatization. However, quick and spontaneous microbial stimulation, as well as sustenance from the hematite and MWCNT reactors was observed, with MWCNT reactors (18–60 h) resulting in a higher sCOD removal efficiency. Following the 72-h mark, hematite reactors reported higher sCOD removal efficiency than the MWCNT and control reactors.

Stimulation of methane gas by hematite and MWCNTs

The success of BSIW degradation process depends on the establishment of syntrophic cooperation between propionate-oxidizing bacteria (or butyrate-oxidizing bacteria, etc.) and the methanogenic archaea that ultimately convert these compounds to methane gas. Degradation of BSIW in the batch bottles began immediately with no observed lag phase, with acetate and propionate reaching peak concentrations within the short span of time of 6 h. This is indicative of robust digestion of BSIW, which might have been assisted by an active biomass. The quick depletions of acetate and propionate in the presence of hematite and MWCNTs could signify their faster and more robust conversion to methane gas (Fig. 2a, b). Bottles supplemented with hematite and MWCNT showed comparatively low acetate quantities compared to the control reactors for approximately 90 h before depletion to less than 1 mg/L. The production and utilization of propionate followed almost the same trend.

Uninterrupted microbial digestion processes might have resulted in a higher methane gas production in the control reactors before 18 h (Fig. 2c). However, a steady improvement in the production of methane gas in the hematite and MWCNT reactors was evident, yielding 37.1, 44.3, and 44.5 mL after 30 h in the control, hematite, and MWCNT reactors, respectively. Thereafter, the hematite reactors produced more CH₄ gas than the MWCNT and control reactors. This culminated in an anaerobic digestion process which enhanced the methane production rate than that in the control reactors by 35 and 20% in the hematite and MWCNT reactors, respectively. Higher biomethanation processes in the presence of hematite can be attributed to its highly conductive characteristics which are due to structural orientation, thermodynamics, and reactivity capabilities that influence the methanogenic response (Zhou et al. 2014), all of which can result in different interaction patterns with the substrate (Navrotsky et al. 2008), while MWCNT was a stable nanomaterial with high electric conductivity and could enhance the syntrophic oxidation rate of butyrate to CH₄ and CO₂ by facilitating the DIET (Zhang and Lu 2016).

Furthermore, it was apparent that the depletion rate of propionate and acetate was congruent with the increase in methane production. The presence of hematite and MWCNTs resulted in a faster reduction of the metabolites, concomitantly producing more CH₄ gas. It is probable that electrons generated from the oxidation of BSIW were transmitted to the methanogens through an electron conduit consisting of arrays of hematite or MWCNTs.

Microbial community analysis

The Shannon index of 3.020, 2.850, and 2.874 (bacteria) and 5.194, 5.354, and 5.276 (archaea) for the control, MWCNTs, and hematite samples, respectively, is an indicator of almost similar microbial diversity in the three types of the reactors. This shows that despite of the use nanoparticles, microbial diversity remained unchanged. In addition, the coverage value of above 96% (bacteria) and 98% (archaea) is a demonstration that the sampling technique tool used was sufficient enough to reflect the community composition in an ecosystem (Liu et al. 2012).

An analysis of the microbial community demonstrated an excess of a 97% predominance of the archaea phylum *Euryarchaeota* (Fig. 3a). On the other hand, bacterial predominance indicated the presence, in order from the most to least dominant, of the phyla *Chloroflexi*, *Proteobacteria*, *Bacteroidetes*, and *Firmicutes* (Fig. 3b). While the influence of nanoparticles upon the abundance of archaea could hardly be recognized, the population of *Chloroflexi* appeared to have declined in the presence of hematite (6.8%) and MWCNTs (6.5%), although the former enriched mostly *Bacteroidetes* (3.6%) whereas the latter slightly enriched *Proteobacteria* (1.2%), *Firmicutes* (1.7%), *Verrucomicrobia* (1.0%), and *Thermotogae* (0.8%).

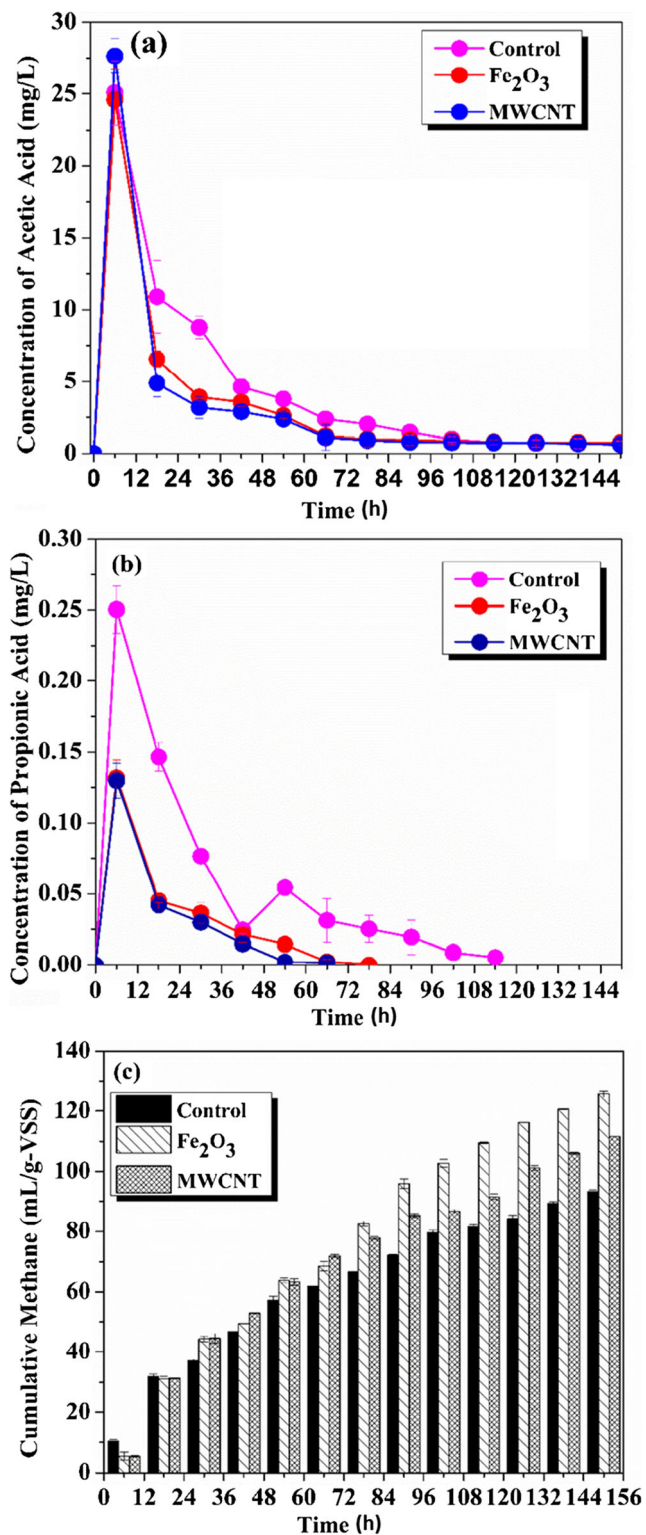


Fig. 2 Changing profiles of **a** acetic acid concentrations, **b** propionic acid concentrations, and **c** methane gas production. Error bars represent the standard deviations resulting from duplicate tests

The predominance of the phylotypes, among the archaea in the class, order, family, and genus, followed the same trend as of the phylum (Fig. 3a). At the order level, there was barely any

difference in the abundance of *Methanosarcinales*, although *Methanobacteriales*' abundance dropped while that of *Methanomicrobiales* slightly increased. Compared to the genus level, this scenario was replicated with *Methanosaeta* (with abundance above 90% in all the reactors) showing no significance difference in the presence of the MWCNTs and hematite. Its predominance was followed by *Methanobacterium* and *Methanolinea* where the former slightly reduced while the later increased in abundance in the presence of MWCNT and hematite.

The bacteria at the class (Fig. 3c) and order (Fig. 3d) level were dominated by *Anaerolineae*, *Deltaproteobacteria*, *Bacteroidia*, and *Clostridia* and *Anaerolineales*, *Bacteroidales*, *Clostridiales*, and *Syntrophobacterales*, respectively, in a descending order. At the order level, while *Anaerolineales* were seen to be at the decrement, *Bacteroidales*, *Clostridiales*, and *Syntrophobacterales* abundance rose slightly in the presence of both MWCNTs and hematite. The family level (Fig. 3e) was dominated by *Anaerolineaceae*, *Porphyromonadaceae*, *Rikenellaceae*, and *Geobacteraceae*. On the other hand, *Anaerolinea*, *Longilinea*, unclassified *Porphyromonadaceae*, *vadinBC27_wastewater-sludge_group*, and *Geobacter* comprised the first five in the genus level (Fig. 3f) in a descending order. In the presence of MWCNT and hematite, unclassified *Porphyromonadaceae* and *vadinBC27_wastewater-sludge_group* increased in abundance while *Anaerolinea*, *Longilinea*, and *Geobacter* reduced.

Furthermore, a search for gene sequences in GenBank revealed that microbes under the *Methanosaeta* genera were related to the species *Methanosaeta concilii*, while those classified under the *Methanobacterium* genera were aligned to *Methanobacterium formicicum*. The bacterial dominance showed sequences aligned to *Anaerolineaceae* bacterium enrichment culture clone B6_178, *Longilinea arvoryzae* and *Geobacter lovleyi* SZ. The predominance of the bacterial species *Anaerolineaceae* (28.6–34.6%) and *Longilinea arvoryzae* (9.1–10.5%) in this study is of significant importance due to their hydrolytic fermentative characteristics in the degradation of cellulosic-related material found in BSIW. They are known to produce cellulosomes, which enhance the degradation of recalcitrant microcrystalline cellulose, while at the same time releasing compounds, such as H₂, CO₂, formate, and acetate, which are eventually utilized by acetogens and methanogens (Lynd et al. 2002). Their presence had the potential for an immense contribution to the oxidation of sucrose to glucose, as well as its subsequent degradation to reduced products for the further reduction of methanogens to CH₄ gas. The success of this process potentially resulted either from the direct transfer of electrons in syntrophic communities by relying on the exchange of diffusible molecules and energy carriers such as hydrogen (or formate) or from the establishment of direct interspecies electron transfer (DIET) among the microbes, with either

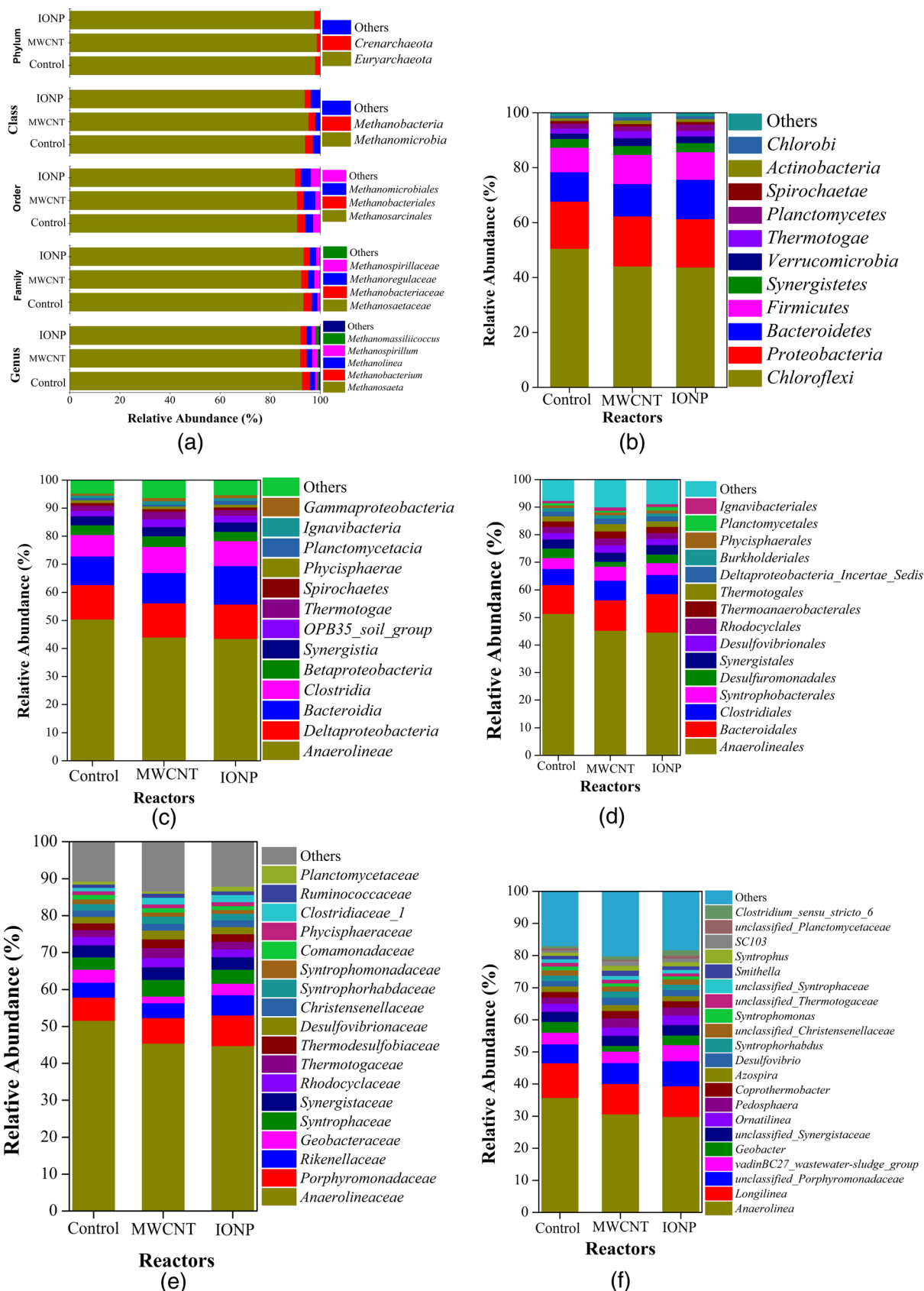


Fig. 3 Taxonomic classification of the dominant phylogenetic groups of the **a** archaea and bacteria, **b** phylum, **c** class, **d** order, **e** family, and **f** genus level (the relative abundance of phyla comprising less than 1% of the total composition in the reactors was defined as “other”)

hematite or MWCNTs serving as electron conduits between acetogens and carbon dioxide-reducing methanogens.

Although *Geobacter* strains are known to enhance DIET with methanogens (Kato et al. 2012a), the presence of the species *Geobacter lovleyi* SZ, which is not known to stimulate DIET, indicates the possibility that there was no direct transfer of electrons among the syntrophic communities. In addition, the low count of the gene sequences of 3.3, 1.7, and 3.0%, which correlate with measured productions of methane gas of 93.2, 111.6, and 125.7 mg/g-VSS for the control, MWCNT, and hematite reactors, respectively, could represent a clear demonstration that the *Geobacter* species may not have acted as a pathway for DIET to methanogens. In fact, their reduction in the presence of MWCNTs and hematite could only have resulted to reduction of the produced methane gas rather than its increment. However, the role of the *Geobacter lovleyi* SZ species in BSIW degradation warrants further investigation.

The process of electron exchange via the indirect electron carriers H₂ and formate is chiefly utilized by the methanogens *Methanobacterium* and *Methanospirillum* (Li et al. 2015a). The sustainability of this process, however, depends mainly on low levels of H₂ maintenance (typically below 10⁻⁵ atm) by H₂-scavenging hydrogenophilic methanogens (Mori and Harayama 2011; Schmidt and Ahring 1995). Although the presence of the *Methanobacterium formicicum* species confirms the role it might have played, i.e., of converting carbon dioxide to methane, in utilizing electrons, the low levels of *Methanobacterium* (below 2%) and *Methanospirillum* microorganisms (below 1%) among all of the reactors are a demonstration that neither H₂ nor formate was a major electron shuttle during methane production. In addition, the quantity of hydrogen gas in this study was often undetected and was thus available in very low quantities, if at all.

Microscopic imaging of anaerobic granular sludge

Figure 4a–c shows the different bacterial structures observed using scanning electron microscopy (SEM). Figure 4a (the control sample) demonstrates the presence of loose and dispersed bacteria compared with the densely packed bacteria in Fig. 4b (hematite) and Fig. 4c (MWCNTs). Figure 4c shows a structure of aggregates creating a gap/fracture, which may entangle microbial flocs, thereby damaging the cells present. This phenomenon could emanate from the physical contact between MWCNTs and bacterial cells and might have resulted in membrane damage, although this might have been an initial stage of cell rupture/damage. This is because, as earlier reported, MWCNTs enhanced the methane production rate as compared to the control reactors, although a little lower compared to hematite. Acute MWCNT piercing might cause cell death, reduced viability, and reduced or absent microbial activity, which is a situation that was not detected during the incubation process.

The densely packed phenomenon can be associated with the interactions among hematite or MWCNTs, microbes, and

induced EPS, which attach on the cell surface to provide a defensive barrier to external interference (Sheng et al. 2010). This protection against external intrusion might have significantly contributed to the enhancement of the methane production rate above the control reactors. The EDS showed peaks of carbon content by weight for the control sample, hematite, and MWCNTs of 51.38, 42.29, and 51.63% and iron contents by weight of 4.33, 21.19, and 7.19%, respectively (Fig. 4d–f). The hematite reactor showed more abundant metal iron, whereas the MWCNT reactor demonstrated more metal carbon than other reactors, an indication that hematite and MWCNTs were still in their respective reactors after successful degradation.

CLSM observations demonstrate EPS spatial distribution in the granular sludge (Fig. 5). Fig. 5 (a1–a3) shows proteins and polysaccharides conforming to granule aggregation and adopting an even distribution pattern. In contrast, Fig. 5 (b1–b3: hematite) and Fig. 5 (c1–c4: MWCNTs) show proteins and α -D- and β -D-glucopyranose polysaccharides forming an outer ring-like layer surrounding the granules. This might be a defensive mechanism against hematite and MWCNT piercing through the membranes of the microbes, hence averting toxicity to microbial consortia due to cell membrane agitation. The SEM and CLSM results clearly demonstrate that protection against cytotoxicity was enhanced by the dense agglomeration of EPS about the microbes, thus forming a formidable protective barrier and the MWCNTs and hematite could not penetrate into the granular layer.

The SEM images of MWCNT granular sludge showed a section of cells experiencing damage. This damage may have resulted in mild toxicity and a slight reduction in microbial metabolic activities, which subsequently resulted in lower methane gas production. Factors that can contribute to multi-wall carbon nanotube toxicity involve oxidative stress, residual catalysts, and cell membrane penetration (Kang et al. 2007; Pasquini et al. 2013). For oxidative stress to induce damage, O₂ is required as a precursor. The anaerobic conditions in this study make this cause insignificant. Meanwhile, carbon nanotubes are known to release impurities that catalyze toxicity. Studies show that impurities released from 40 to 60% pure single wall carbon nanotubes demonstrated negligible toxicity effects (Liu et al. 2007; Tong et al. 2012). The use of 97% purity MWCNTs diminished the possibility of the release of catalyst metals that could trigger inhibitory effects.

Therefore, cell membrane perturbation due to the physical interaction between bacterial cells and MWCNTs could be a possible cause of toxicity because the reactors were always in motion on a mechanical shaker during incubation. In a recent study where MWCNTs were used in an expanded granular sludge bed reactor, cell perturbation was not evidenced (Ambuchi et al. 2017). This shows that MWCNTs can induce microbial activity without resulting to toxicity. However, the damage inflicted might have been at its initial stage of cell breakage. On the other hand, this may not have resulted in severe damage because the CLSM demonstrated EPS forming

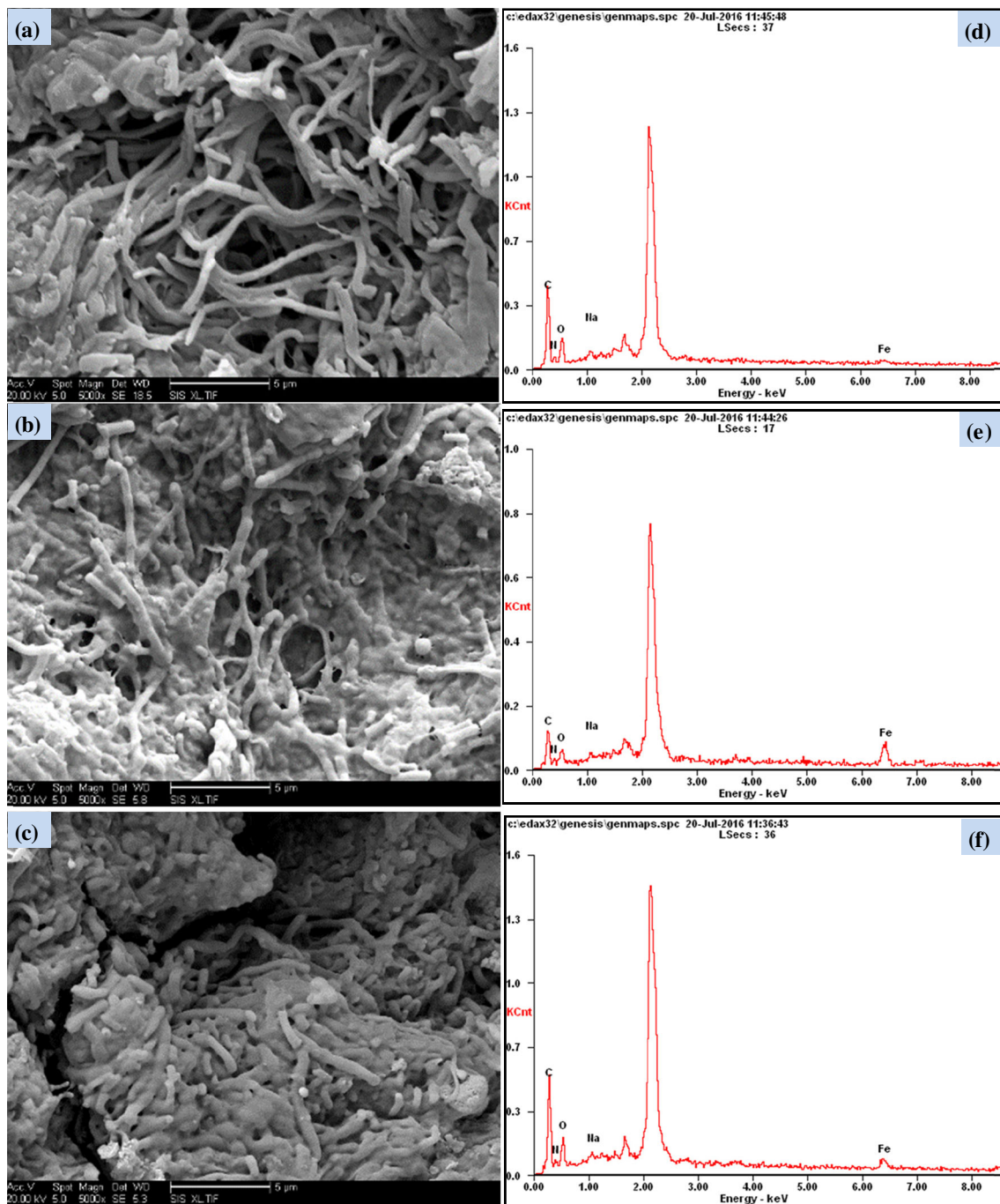


Fig. 4 SEM images (a–c) and EDS plots (d–f) of sludge in different reactors. **a, d** Control. **b, e** Hematite. **c, f** MWCNT

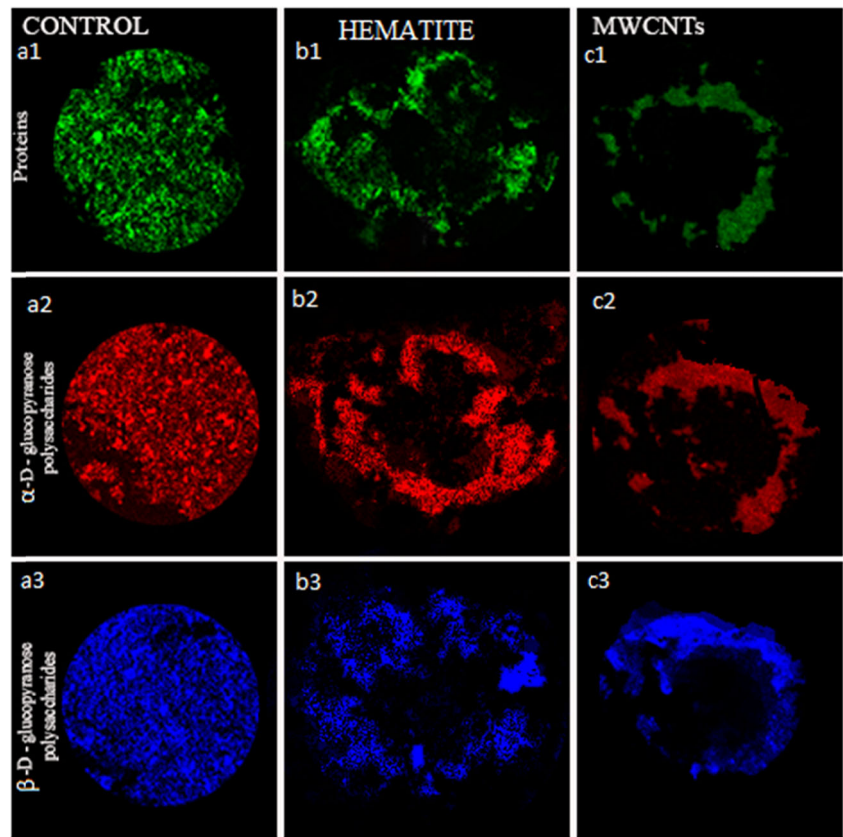
a protective layer around the microbial cells against harsh external environmental influence. This could partly explain the stimulation of the higher production of CH_4 gas for hematite compared to that for MWCNTs.

Discussion

In this study, hematite and MWCNT reactors produced substantially higher methane gas in comparison to the control reactors. It

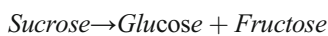
is thus probable that the conversion rate of BSIW to methane gas was greatly influenced. Although the influence of hematite and MWCNTs resulted into the reduction and or enrichment in microbial community, to a large extent, this influence could barely be translated into CH_4 gas enhancement. For instance, if the enrichment of microbial community could directly influence microbial activity, then the reduction of *Anaerolinea* (5.1 and 5.9% in MWCNT and hematite reactors, respectively) and *Longilinea* (1.3% in both MWCNT and hematite reactors) could have resulted to subsequent higher performance in the control reactors as

Fig. 5 Profiles of EPS in the granular sludge from the control (a1-a3), hematite (b1-b3), and MWCNT (c1-c3) exposed reactors. The sludge granules were stained with FITC (proteins: a1, b1, and c1), Con A (α -D-glucopyranose polysaccharides: a2, b2, and c2), and calcofluor white (β -D-glucopyranose polysaccharides: a3, b3 and c3)



opposed to hematite and MWCNT reactors, of which, it was not. The *Anaerolinea* and *Longilinea* bacteria are known to play a significant role in the degradation of cellulosome in BSIW releasing compounds that can be utilized by methanogens in the formation of CH_4 gas. Recently, the enrichment of *Anaerolinea* in the presence of hematite and MWCNTs in a continuous experiment still realized increment in methane gas (Ambuchi et al. 2017). In addition, the *Methanosaeta* genera which plays syntrophic role with the bacteria depicted no significance difference in the presence of hematite and MWCNTs. This is an utter demonstration that besides the enrichment of the microbial community, hematite and MWCNT assume a different role which increases CH_4 gas production.

Anaerobic degradation of sucrose, which is the main carbon in the BSIW, is facilitated by microbial activity and might have been enhanced by use the hematite and MWCNTs. The first step in fermentation is the breaking down of sucrose into its components:

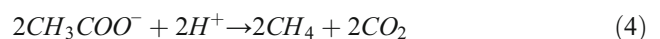
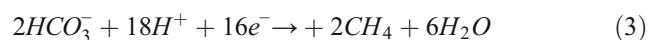
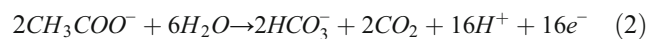


Fructose is further converted by enzyme isomerase to glucose



Glucose is the starting substrate of the glycolytic pathway. This is hydrolyzed by the homoacetogenic bacteria

(*Anaerolinea* and *Longilinea*-as depicted from this study) resulting into 2 mols of acetate per mole of glucose as shown in reaction (1). Acetate is oxidized producing HCO_3^- and H^+ (2). The methanogens (*Methanosaeta*) obtain electrons and convert H^+ and HCO_3^- to CH_4 (3). The hematite and MWCNTs in this study might have enabled the syntrophic microorganisms to share the produced electrons directly, enhancing CH_4 gas production. However, there were other reactions that most likely contributed to methane gas formation, for example, the reaction between hydrogen and carbon dioxide (5). As earlier noted, this could be the reason for the production of scant amount of hydrogen. This resulted to the overall reaction (6)



The overall reaction is



However, the amounts of CH_4 gas ultimately produced from the degradation of BSIW, which were roughly 2.22 and 2.20 mol of methane per mol of glucose (after conversion

from sucrose) that was consumed due to the influences of hematite and MWCNTs, respectively, were slightly lower than the value predicted from the stoichiometric calculations of the classical methanogenic glucose degradation pathway of 3 mol of methane produced per mol of glucose consumed ($C_6H_{12}O_6 \rightarrow 3CH_4 + 3CO_2$). The deficit may be equivalent to the amount diverted to facilitate biomass growth (Siegrist et al. 2002). This characteristic is not uncommon with this inoculum, which has a low quantity of alternative electron acceptors, such as nitrate and sulfate. Furthermore, there was very low production of carbon dioxide than the expected 3 mol. The abundance of the calcium ions (Ca^{2+}) in the substrate due to the use of lime during industrial beet sugar processing could be the reason, as shown in Table 1 ($225.55 \pm 0.72 \text{ mg L}^{-1}$) and the use of lime when regulating the pH of the substrate (Iza et al. 1990). The use of lime in beet sugar processing industries aids in adjusting of the pH and enhance settling characteristics. Its reaction with carbon dioxide results to bicarbonate alkalinity [$Ca(HCO_3)_2$] and precipitates ($CaCO_3$). This reaction results to the loss of carbon dioxide in the sludge, of which carbon dioxide from the biogas is its replacement (Gerardi 2003). This might have resulted into very low carbon dioxide composition of the biogas.

The abundance of *Methanosaeta concilii* in this study might have exerted a twofold influence on the production of CH_4 gas. As an acetate-utilizing methanogen, it is implied that it was able to convert acetate directly to CH_4 gas at the moment of its production. This can explain the process of methane gas production in the reactors, insomuch that it was potentially the major process in the control reactors that lacked NPs. Apart from utilizing acetate, *Methanosaeta* species have the ability to directly accept electrons as an electron donor for the reduction of carbon dioxide to CH_4 gas; they have been known to directly accept electrons from a conductive aggregate matrix (Morita et al. 2011). Because of this, hematite and MWCNTs might have been utilized as conduits for the transfer of electrons from *Anaerolinea* and *Longilinea* to *Methanosaeta* species. Therefore, hematite and MWCNTs might have contributed to the increase in methane gas by 35 and 20%, respectively.

These findings, hematite and carbon nanotubes can promote DIET among syntrophic microbial communities, represent a novel function for nanoparticle use, as well as an essentially unexplored area of technological importance with relevance to industrial and environmental sectors. Even though the use of hematite and MWCNTs could have negative effects to the microbial community, this study, through the use of SEM and CLSM, demonstrated that there was visible interaction between microbes, hematite, or MWCNTs and EPS, with the later promoting a formidable defense against external intrusion. This defensive mechanism might have contributed to a larger extend to higher methane production rate among the reactors with hematite

and MWCNTs in comparison to the control. Thus, this study illustrates that use of hematite and MWCNTs in the treatment of BSIW resulted in an increase in the production of methane gas, evidence that the existing anaerobic digestive systems have the potential for further improving methane gas generation by enhancing DIET. This study supports the recent findings where hematite and MWCNTs enhanced CH_4 gas production in a continuous experiment (Ambuchi et al. 2017) and indeed adds more into the evidence of DIET enhancement mechanism especially by MWCNTs which had not been associated with before.

The addition MWCNTs may represent a novel and unexplored strategy for promoting DIET in the process of improving the production of methane gas in the anaerobic biodegradation process, which has enormous potential for harnessing biofuels. The results presented herein could have broad impacts in the renewable energy biotechnology sector, wastewater treatment plants, and industries and beet sugar processing factories.

In summary, the enhancement of the production of CH_4 gas using hematite and MWCNT in a batch experiment was investigated in this study. There was higher rate of substrate degradation in the presence of hematite and MWCNTs which resulted into higher COD removal rate than the control. Besides, production of CH_4 gas was enhanced by 35% with the use of hematite and 20% in the presence of MWCNT. This stimulation might have resulted from hematite and MWCNTs acting as conduits for interspecies electron transfer between the homoacetogenic bacteria and methanogens. Different microbial community enrichment levels were also observed even as *Anaerolinea* and *Longilinea* genus slightly reduced while unclassified *Porphyromonadaceae* genera increased among the bacteria in the presence of hematite and MWCNTs. Among the methanogens, there was no observed significant difference among the *Methanosaeta* genera, although *Methanobacterium* genera slightly reduced while *Methanolinea* genera increased in abundance. However, the enrichment of microbial community was most unlikely a contributing factor to CH_4 gas enhancement.

Funding This work was supported by the National Key Research and Development Program of China (2016YFC0401106), the National Science Foundation of China (51308150, 51125033), the Fundamental Research Funds for the Central Universities (HIT. MKSTISP. 2016 14), and the State Key Laboratory of Urban Water Resource and Environment (Harbin Institute of Technology, 2016TS05).

Compliance with ethical standards

Conflict of interest The authors declare that they have no conflict of interest.

Ethical approval This article does not contain any studies with human participants or animals performed by any of the authors.

References

- Ambuchi JJ, Zhang ZH, Shan LL, Liang DD, Zhang P, Feng YJ (2017) Response of anaerobic granular sludge to iron oxide nanoparticles and multi-wall carbon nanotubes during beet sugar industrial wastewater treatment. *Water Res* 117:87–94. <https://doi.org/10.1016/j.watres.2017.03.050>
- Angelidaki I, Sanders W (2004) Assessment of the anaerobic biodegradability of macropollutants. *Rev Environ Sci Biotechnol* 3:117–129. <https://doi.org/10.1007/s11157-004-2502-3>
- Antoni D, Zverlov VV, Schwarz WH (2007) Biofuels from microbes. *Appl Microbiol Biotechnol* 77(1):23–35. <https://doi.org/10.1007/s00253-007-1163-x>
- Aulenta F, Rossetti S, Amalfitano S, Majone M, Tandoi V (2013) Conductive magnetite nanoparticles accelerate the microbial reductive dechlorination of trichloroethene by promoting interspecies electron transfer processes. *Chemosuschem* 6(3):433–436. <https://doi.org/10.1002/cssc.201200748>
- Bastviken D, Tranvik LJ, Downing JA, Crill PM, Enrich-Prast A (2011) Freshwater methane emissions offset the continental carbon sink. *Science* 331(6013):50–50. <https://doi.org/10.1126/science.1196808>
- Boone DR, Johnson RL, Liu Y (1989) Diffusion of the interspecies electron carriers H₂ and formate in methanogenic ecosystems and its implications in the measurement of km for H₂ or formate uptake. *Appl Environ Microbiol* 55(7):1735–1741
- Gerardi MH (2003) *The microbiology of anaerobic digesters*. John Wiley & Sons, Inc, Hoboken
- Iza J, Palencia JI, Fdzpolanco F (1990) Waste-water management in a sugar-beet factory—a case-study of comparison between anaerobic technologies. *Water Sci Technol* 22(9):123–130
- Kang S, Pinaut M, Pfefferle LD, Elimelech M (2007) Single-walled carbon nanotubes exhibit strong antimicrobial activity. *Langmuir* 23(17):8670–8673. <https://doi.org/10.1021/la701067r>
- Kato S, Hashimoto K, Watanabe K (2012a) Methanogenesis facilitated by electric syntrophy via (semi)conductive iron-oxide minerals. *Environ Microbiol* 14(7):1646–1654. <https://doi.org/10.1111/j.1462-2920.2011.02611.x>
- Kato S, Hashimoto K, Watanabe K (2012b) Microbial interspecies electron transfer via electric currents through conductive minerals. *Proc Natl Acad Sci U S A* 109(25):10042–10046. <https://doi.org/10.1073/pnas.1117592109>
- Li HJ, Chang JL, Liu PF, Fu L, Ding DW, Lu YH (2015a) Direct interspecies electron transfer accelerates syntrophic oxidation of butyrate in paddy soil enrichments. *Environ Microbiol* 17(5):1533–1547. <https://doi.org/10.1111/1462-2920.12576>
- Li LL, Tong ZH, Fang CY, Chu J, Yu HQ (2015b) Response of anaerobic granular sludge to single-wall carbon nanotube exposure. *Water Res* 70:1–8. <https://doi.org/10.1016/j.watres.2014.11.042>
- Liu XY, Gurel V, Morris D, Murray DW, Zhitkovich A, Kane AB, Hurt RH (2007) Bioavailability of nickel in single-wall carbon nanotubes. *Adv Mater* 19(19):2790–2796. <https://doi.org/10.1002/adma.200602696>
- Liu FH, Rotaru AE, Shrestha PM, Malvankar NS, Nevin KP, Lovley DR (2012) Promoting direct interspecies electron transfer with activated carbon. *Energy Environ Sci* 5(10):8982–8989. <https://doi.org/10.1039/c2ee22459c>
- Lynd LR, Weimer PJ, van Zyl WH, Pretorius IS (2002) Microbial cellulose utilization: fundamentals and biotechnology. *Microbiol Mol Biol Rev* 66(3):506–577. <https://doi.org/10.1128/Mmbr.66.3.506-577.2002>
- Mori K, Harayama S (2011) *Methanobacterium petrolearium* sp. nov. and *Methanobacterium ferruginis* sp. nov., mesophilic methanogens isolated from salty environments. *Int J Syst Evol Microbiol* 61:138–143. <https://doi.org/10.1099/ijs.0.022723-0>
- Morita M, Malvankar NS, Franks AE, Summers ZM, Giloteaux L, Rotaru AE, Rotaru C, Lovley DR (2011) Potential for direct interspecies electron transfer in methanogenic wastewater digester aggregates. *Mbio* 2(4):e00159–e00111. <https://doi.org/10.1128/mBio.00159-11>
- Nagarajan H, Embree M, Rotaru AE, Shrestha PM, Feist AM, Palsson BO, Lovley DR, Zengler K (2013) Characterization and modelling of interspecies electron transfer mechanisms and microbial community dynamics of a syntrophic association. *Nat Commun* 4:2809. <https://doi.org/10.1038/Ncomms3809>
- Navrotsky A, Mazeina L, Majzlan J (2008) Size-driven structural and thermodynamic complexity in iron oxides. *Science* 319(5870):1635–1638. <https://doi.org/10.1126/science.1148614>
- Pasquini LM, Sekol RC, Taylor AD, Pfefferle LD, Zimmerman JB (2013) Realizing comparable oxidative and cytotoxic potential of single- and multiwalled carbon nanotubes through annealing. *Environ Sci Technol* 47(15):8775–8783. <https://doi.org/10.1021/es401786s>
- Rotaru AE, Shrestha PM, Liu FH, Shrestha M, Shrestha D, Embree M, Zengler K, Wardman C, Nevin KP, Lovley DR (2014) A new model for electron flow during anaerobic digestion: direct interspecies electron transfer to *Methanosaeta* for the reduction of carbon dioxide to methane. *Energy Environ Sci* 7(1):408–415. <https://doi.org/10.1039/c3ee42189a>
- Schink B (1997) Energetics of syntrophic cooperation in methanogenic degradation. *Microbiol Mol Biol Rev* 61(2):262–280
- Schmidt JE, Ahring BK (1995) Interspecies electron-transfer during propionate and butyrate degradation in mesophilic, Granular Sludge. *Appl Environ Microbiol* 61(7):2765–2767
- Sheng GP, Yu HQ, Li XY (2010) Extracellular polymeric substances (EPS) of microbial aggregates in biological wastewater treatment systems: a review. *Biotechnol Adv* 28(6):882–894. <https://doi.org/10.1016/j.biotechadv.2010.08.001>
- Siegrist H, Vogt D, Garcia-Heras JL, Gujer W (2002) Mathematical model for meso- and thermophilic anaerobic sewage sludge digestion. *Environ Sci Technol* 36(5):1113–1123. <https://doi.org/10.1021/es010139p>
- Smith M, Mah R (1978) Growth and methanogenesis by *Methanosarcina* strain 227 on acetate and methanol. *Appl Environ Microbiol* 36(6):870–879
- Stams AJM, Plugge CM (2009) Electron transfer in syntrophic communities of anaerobic bacteria and archaea. *Nat Rev Microbiol* 7(8):568–577. <https://doi.org/10.1038/nrmicro2166>
- Stams AJM, de Bok FAM, Plugge CM, van Eekert MHA, Dolfing J, Schraa G (2006) Exocellular electron transfer in anaerobic microbial communities. *Environ Microbiol* 8(3):371–382. <https://doi.org/10.1111/j.1462-2920.2006.00989.x>
- Thiele JH, Zeikus JG (1988) Control of interspecies electron flow during anaerobic-digestion—significance of formate transfer versus hydrogen transfer during syntrophic methanogenesis in flocs. *Appl Environ Microbiol* 54(1):20–29
- Tong ZH, Bischoff M, Nies LF, Myer P, Applegate B, Turco RF (2012) Response of soil microorganisms to as-produced and functionalized single-wall carbon nanotubes (SWNTs). *Environ Sci Technol* 46(24):13471–13479. <https://doi.org/10.1021/es303251r>
- Viggi CC, Rossetti S, Fazi S, Paiano P, Majone M, Aulenta F (2014) Magnetite particles triggering a faster and more robust syntrophic pathway of methanogenic propionate degradation. *Environ Sci Technol* 48(13):7536–7543. <https://doi.org/10.1021/es5016789>
- Wang J, Zhang ZJ, Zhang ZF, Qaisar M, Zheng P (2007) Production and application of anaerobic granular sludge produced by landfill. *J Environ Sci (China)* 19(12):1454–1460. [https://doi.org/10.1016/S1001-0742\(07\)60237-X](https://doi.org/10.1016/S1001-0742(07)60237-X)
- Zhang JC, Lu YH (2016) Conductive Fe₃O₄ nanoparticles accelerate syntrophic methane production from butyrate oxidation in two different lake sediments. *Front Microbiol* 7. <https://doi.org/10.3389/Fmicb.2016.01316>

- Zhang Z, Gao P, Cheng J, Liu G, Zhang X, Feng Y (2018) Enhancing anaerobic digestion and methane production of tetracycline wastewater in EGSB reactor with GAC/NZVI mediator. *Water Res* 236: 54–63. <https://doi.org/10.1016/j.watres.2018.02.025>
- Zhou SG, Xu JL, Yang GQ, Zhuang L (2014) Methanogenesis affected by the co-occurrence of iron(III) oxides and humic substances. *FEMS Microbiol Ecol* 88(1):107–120. <https://doi.org/10.1111/1574-6941.12274>
- Zhuang L, Tang J, Wang YQ, Hu M, Zhou SG (2015) Conductive iron oxide minerals accelerate syntrophic cooperation in methanogenic benzoate degradation. *J Hazard Mater* 293:37–45. <https://doi.org/10.1016/j.jhazmat.2015.03.039>